

# Fragmentation and Mineralization of a Compostable Aromatic–Aliphatic Polyester during Industrial Composting

Wendel Wohlleben,\* Markus Rückel, Lars Meyer, Patrizia Pfohl, Glauco Battaglia, Thorsten Hüffer, Michael Zumstein, and Thilo Hofmann



Cite This: <https://doi.org/10.1021/acs.estlett.3c00394>



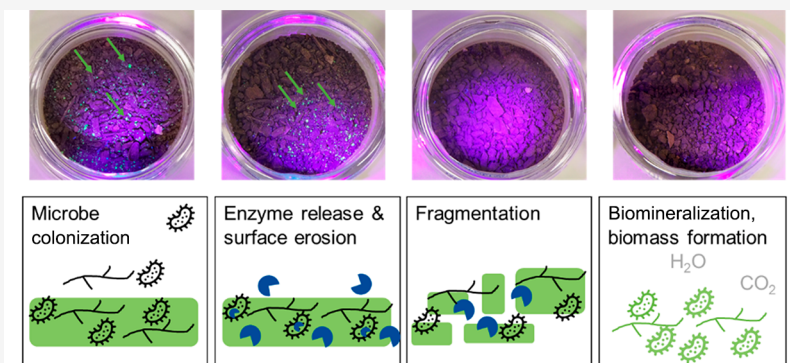
Read Online

ACCESS |

Metrics & More

Article Recommendations

Supporting Information



**ABSTRACT:** Compostable plastics support the separate collection of organic waste. However, there are concerns that the fragments generated during disintegration might not fully biodegrade and leave persistent microplastic in compost. We spiked particles of an aromatic–aliphatic polyester containing polylactide into compost and then tracked disintegration under industrial composting conditions. We compared the yields against polyethylene. The validity of the extraction protocol and complementary microscopic methods ( $\mu$ -Raman and fluorescence) was assessed by blank controls, spike controls, and prelabeled plastics. Fragments of 25–75  $\mu\text{m}$  size represented the most pronounced peak of interim fragmentation, which was reached already after 1 week of industrial composting. Larger sizes peaked earlier, while smaller sizes peaked later and remained less frequent. For particles of all sizes, count and mass decreased to blank level when 90% of the polymer carbon were transformed into  $\text{CO}_2$ . Gel permeation chromatography (GPC) analysis suggested depolymerization as the main driving force for disintegration. A transient shift of the particle composition to a lower percentage of polylactide was observed. Plastic fragmentation during biodegradation is the expected route for decomposing, but no accumulation of particulate fragments of any size was observed.

**KEYWORDS:** *Microplastics, Biodegradation, Fragmentation, Persistence, Composting*

## INTRODUCTION

According to the European Environmental Agency, 34% of the municipal waste in the EU consisted of biowaste in 2020.<sup>1</sup> Being the largest single component in European municipal waste, if utilized properly, biowaste has a high potential to contribute to a circular economy by delivering valuable soil-improvers like compost, as well as biogas, a source of renewable energy. Certified compostable plastics are developed for specific applications where there is a benefit in using them.<sup>2</sup> Compostable plastics could enable diverting organic wastes from landfill and incineration, reducing plastic contamination in the organic waste stream and with that support the goals of the EU Green Deal.<sup>3,4</sup> Certified industrially compostable plastics are designed to deliver performance during application, e.g., as food packaging or as bags for biowaste collection, and to biodegrade in their intended end of life.<sup>2,3,5</sup> The inevitable loss of structural integrity of a plastic article *during composting*

incurs a potential to disintegrate into micro- and nanoplastic fragments, also as an interim phase of biodegradation.<sup>6–13</sup> Studies have investigated the presence of fragments from both conventional and biodegradable plastics in compost or soil.<sup>14–16</sup> However, systematic studies with blank and spike controls are still missing. Protocols developed for characterization of conventional microplastics<sup>17</sup> require validation and possibly adaptation for soil-biodegradable and compostable plastics, because these plastics may inadvertently degrade during the sample preparation procedures.<sup>18,19</sup> In summary,

Received: June 9, 2023

Revised: June 27, 2023

Accepted: June 28, 2023

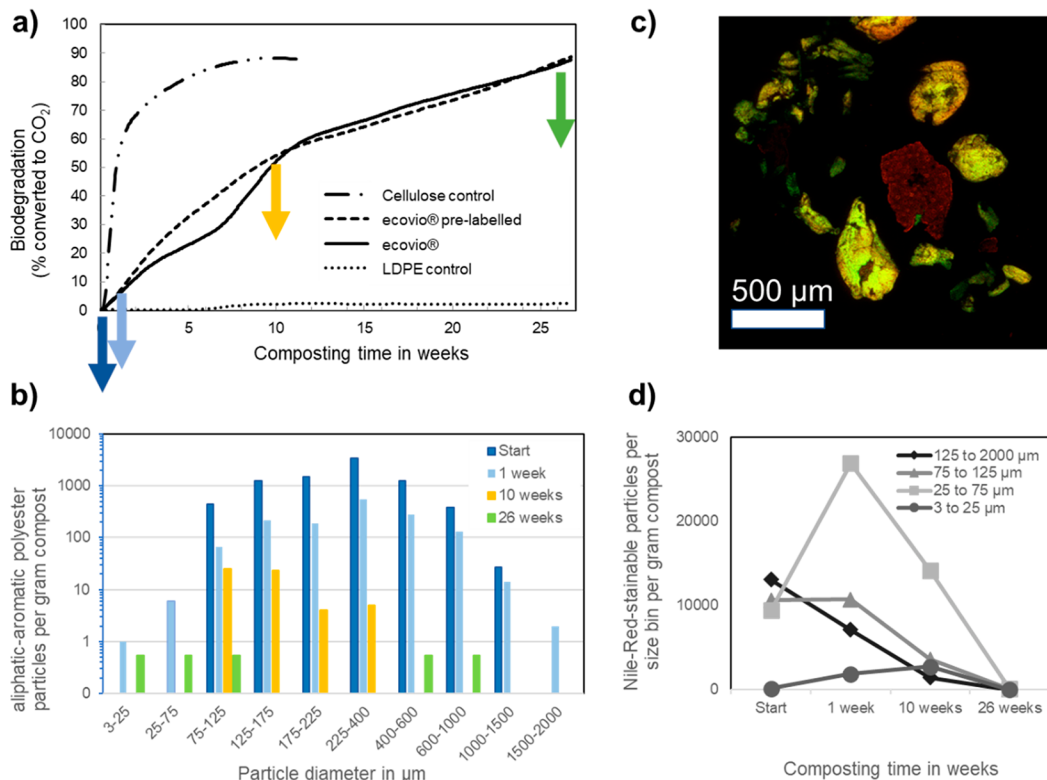


**Figure 1.** Fragmentation kinetics. (a) Biodegradation tracked via CO<sub>2</sub> evolution of aromatic–aliphatic polyester (ecovio) (solid line), prelabelled polyester (dashed), cellulose (dash-dot), and LDPE (dot). Replicates were sacrificed for fragment analysis at the indicated sampling time points (arrows). (b) Chemically selective particle size distribution of fragments of aromatic–aliphatic polyester by  $\mu$ -Raman microscopy. (c) Overlay of red (Nile red) and green (Lumogen yellow) fluorescence from extracted prelabelled polyester, additionally stained by Nile red. One particle in the center appears only red and therefore is part of the compost matrix (see Figure S5 for count and size distributions by either label). (d) Fluorescence microscopy (Nile red) particle counts per size and time.

certified compostable materials have proven to positively impact the amount of biowaste collected and its quality,<sup>20–22</sup> but their interim fragmentation must be addressed properly.

Here, biodegradation-induced fragments were systematically tested using several complementary methods with appropriate controls (i.e., with blank controls, spike controls, and prelabel controls). CO<sub>2</sub> evolution, size distribution, and composition of a certified industrially compostable plastic consisting of an aromatic–aliphatic polyester compound with polylactide (PLA) were tracked.<sup>2,23</sup> We focused on aerobic composting. Findings were compared against low-density polyethylene (LDPE) as the most relevant conventional plastic.<sup>10</sup> Improving from our recent work on polyurethane fragmentation in compost,<sup>18</sup> oxidation- and density-based particle extraction,<sup>17,24</sup> Raman microscopy ( $\mu$ -Raman), and fluorescence microscopy were combined to quantify the temporal evolution of fragments down to a few µm in size with chemical specificity on about 200,000 particles in total. Soxhlet extraction with gel permeation chromatography (GPC) analysis additionally tracked polymer chain scission for the entire polymer content in the compost and selectively for the remaining fragments.

## METHODS AND MATERIALS

**Materials.** Microcrystalline cellulose was purchased from Merck (CAS Number 9004-34-6). LDPE Lupolen 1800 S was purchased from LyondellBasell. The compostable plastic is commercially available from BASF (ecovio PS 1606) and is a compound of PLA with aromatic–aliphatic-polyester. A prelabelled version, needed for initial spiking controls, was

produced by blending 3 kg of ecovio PS 1606 with 3 g of Lumogen F Yellow 083 at 180 °C on a mini-extruder Rheomex CTW 100. All granules were cryo-milled (Retsch ZM 200) with a sieving cutoff of 0.5 mm and dried in a vacuum oven at 36 °C for 48 h.

**Composting.** Biodegradation experiments were performed under industrial composting conditions according to ISO 14855.<sup>25</sup> An 80 g sample of material was composted in 1200 g of compost (OWS Belgium) at 58 ± 2 °C (details in the Supporting Information). The CO<sub>2</sub> evolution in replicate incubation remained within 3% (Figure S1). The graphic in the abstract shows samples of compost with prelabelled ecovio fragments at the start and at 1, 10, and 26 weeks under UV light.

**Extraction: Density-Based Fragment Method with  $\mu$ -Raman and Fluorescence Microscopy.** The extraction consisted of multiple steps (Figure S2), which were individually checked for compatibility with the polymer: (1) Homogenization by tumbler, (2) deagglomeration of 1 g of compost by sonication, (3) organic matrix removal by Fenton oxidation, (4) deagglomeration by sonication, and (5) density separation in 1.4 g/cm<sup>3</sup> ZnCl<sub>2</sub> (Bernd Kraft). By the Stokes–Einstein law, step 5 imposes a lower detectable limit of the 3 µm particle size. The extraction efficiency of 78.2 ± 3.5% was determined by spike and blank controls as described in the Supporting Information. For confocal Raman microscopy (WITec alpha 300R with 785 nm laser, 30 mW, 20x objective), samples were transferred on dried filters. Raman image acquisition and analysis used Suite FIVE and Particle Scout

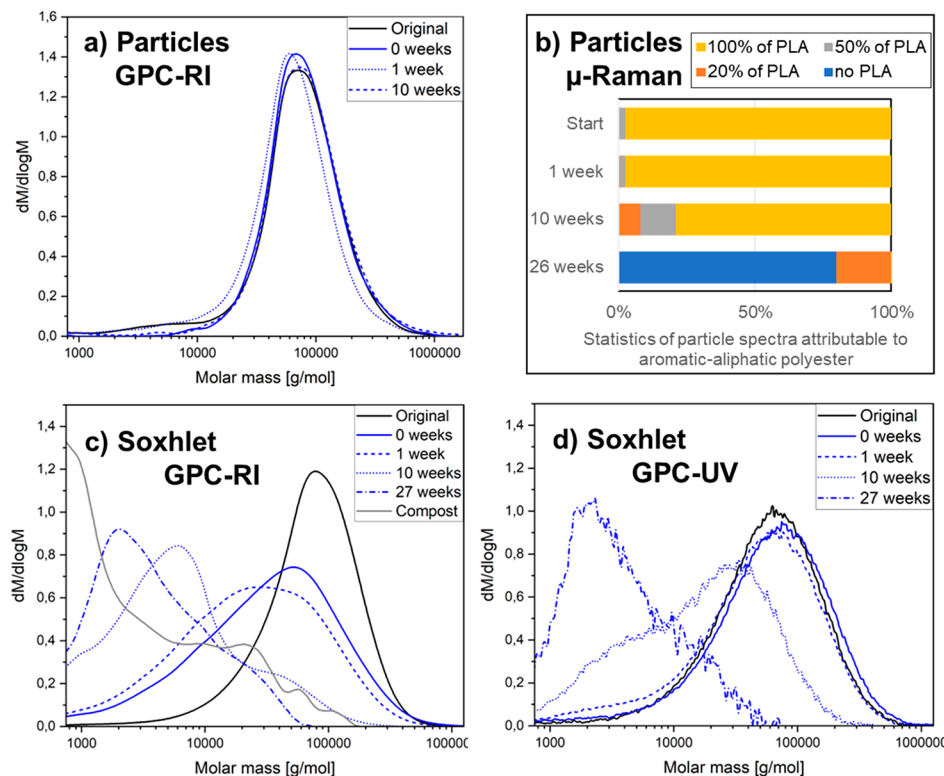


**Figure 2.** Biodegradation on molecular level: (a) normalized molar mass distributions (GPC) of polymer in remaining particles only (from density extraction), compared to (c and d) the entire polymer (from Soxhlet extraction). (b) Chemical identity of the copolymer composition ( $\mu$ -Raman microscopy, summarized in Tables S3–S5) of polymer in remaining particles, concomitant with the reduction of number count in Figure 1b.

software. For fluorescence microscopy, samples were filtered on a Fluoropore Membrane Filter, 1.0  $\mu\text{m}$  pore size, hydrophobic PTFE (FALP02500), stained on the filter by 3 mL of ethanol with 500 ppm of Nile red (30 min), rinsed by pure ethanol, and dried while preventing agglomeration. More than 10,000 particles were characterized for each compost. Lumogen Yellow dye, needed for initial method validation, may migrate or degrade; the reported fragmentation kinetics relied on composting of the pure polymer with Nile red staining *after* extraction. More details on extraction, sample preparation, and microscopy are given in the Supporting Information.

**Extraction: Solvent-Based Soxhlet Method with GPC.** Compost (5 g) was added to an extraction thimble (MN 649, 33  $\times$  94 mm, Macherey-Nagel). A 200 mL aliquot of hexafluoroisopropanol (HFIP, Apollo Scientific) was used to dissolve the polymer (120 °C, 35 cycles), while compost remained in the extraction thimble. After extraction, the solvent was removed in *vacuo*, and the sample was dried overnight (60 °C, *vacuo*). Alternatively, particles that were first extracted by the density-based method were then dissolved in HFIP. The molar mass distributions were determined by GPC (PL HFIPgel columns, 3–100  $\mu\text{m}$ , Agilent) as described earlier<sup>19</sup> and documented in the Supporting Information.

## RESULTS AND DISCUSSION

The fragmentation process was investigated using biodegradation experiments under industrial composting conditions allowing for tracking the evolved carbon dioxide (Figure 1a) and thus sampling at precise degrees of mineralization. The mineralization curve for the positive control cellulose was consistent with that of historical controls. The curves for

ecovio PS1606 and prelabeled ecovio exhibited a deviation between 3 and 10 weeks, attributed to the thermal degradation of PLA during compounding with the dye. Note that fragmentation kinetics in Figures 1 and 2 report the environmentally relevant case without that prelabeling process (see also Methods and Materials). Mineralization rates were strongly impacted by the large particle size of the micronized material, which is an order of magnitude higher than that of the 25  $\mu\text{m}$  thin films used for paper coatings (e.g., for compostable cup application). From 60% mineralization, both curves transitioned into a linear phase instead of reaching a plateau. This behavior was attributed to three possible factors: (1) fast uptake of the polymeric carbon into biomass, which was then slowly mineralized; (2) rate-limiting surface erosion process, or (3) a consequence of fast PLA hydrolysis in the initial stage transitioningally inhibiting metabolism due to locally acidic pH. During the same process, the negative control LDPE was not degraded (Figure 1a, dotted line), as expected.

Four sampling points were linked to key phases of the biodegradation process: at the start, at 1 week (about 6% mineralization), at 10 weeks (50% mineralization), and finally at 26 weeks (90% mineralization).

For fragment extraction, we tested very gentle processes with olive oil<sup>26</sup> on partially biodegraded PU-polyester,<sup>18</sup> but biodegradation diminished the hydrophobicity of the polymer as driving force for extraction efficiency. Here, we combined sonication to deaggregate plastic fragments attached to other compost particles, oxidation to remove the organic background and to ensure proper identification by Raman spectra, and density separation to remove Fenton residue and compost inorganic components (Figure S2).<sup>17,27</sup> We had

previously shown that the particle size distribution, the surface texture and the surface chemistry of the investigated aromatic-aliphatic polyester was not affected.<sup>19</sup> In the blank compost, we found mostly compost fragments with no specific Raman spectrum (attributed to autofluorescent lignin-rich particles, silicates, and fatty acid esters) and fragments of polypropylene, polyethylene, Teflon, and polystyrene (Table S1). Sonication did not significantly change the particle size distribution of the fragments (Figure S3). Several protocols support using sonication for deagglomeration.<sup>17,27,28</sup> The applicability of the acidic density separation medium ZnCl<sub>2</sub> was checked:<sup>29</sup> Partially (1 week) composted polymer was analyzed immediately after extraction, then reanalyzed after 1 month of storage in the ZnCl<sub>2</sub>-based extract, and gave the same results (Figure S4).

To construct the fragmentation kinetics, the results of particle extraction and  $\mu$ -Raman analysis were binned by size and chemical composition (Tables S2–S5), of which Figure 1b shows for each sampling time the size distribution of fragments identified as aromatic-aliphatic polyester per compost mass. At the start of composting, the number of fragments were on par (nearly 10,000 per gram compost) for LDPE and ecovio polymer, whereas after 26 weeks, the ecovio fragment count decreased by 3 orders of magnitude to  $3 \pm 3$  per gram (Figure 1b, green bars show the size distribution of the replicate with a total count of 5 particles). This final count is not significant against the blank count at  $5 \pm 5$  per gram (Table S1). The results are consistent with the biomineralization of 90% of the plastic carbon to CO<sub>2</sub> (Figure 1a) and additionally show the reduction of detectable particles to the blank level. In contrast, the LDPE count decreased only by 7%, which is not significant against the uncertainty in duplicate analysis.

$\mu$ -Raman microscopy is highly selective for polymer types and has a better spatial resolution than infrared microscopy, but is still limited in this regard.<sup>30</sup> Fluorescence microscopy improves the spatial resolution and retains rudimentary specificity by Nile red staining.<sup>28,31</sup> However, Nile red may have stained naturally present compost particles or other microplastic that would thus contribute to the particle count. We hence prelabeled the same aromatic-aliphatic polyester by a fluorescent dye (Lumogen Yellow). The overlay of fluorescence by prelabeling with Lumogen yellow and postlabeling with Nile red (Figures S5a and 1c), and the excellent match of the respective size distributions (Figure S5b) demonstrated sufficient specificity. The analysis of fragmentation kinetics by fluorescence microscopy revealed the size-dependent behavior clearer than that by  $\mu$ -Raman microscopy (Figure 1d): The largest fractions (125–2000  $\mu$ m) decayed monotonously from the beginning; the fraction of 75–125  $\mu$ m stagnated initially and decayed only after 1 week; the fraction of 25–75  $\mu$ m tripled the count from the start to 1 week and then decayed; the smallest detectable fraction of 3–25  $\mu$ m continued to increase up to 10 weeks and then decayed. All fractions returned to the baseline at 26 weeks (Figure 1d). A continuous redistribution from larger to smaller sizes was also observed by Accinelli et al. in soil,<sup>32</sup> but there the final phases of degradation were not followed as done here.

The intermittent generation of particles in the 25–75  $\mu$ m size bin exceeds the losses of larger particles and thus is attributed to their fragmentation, not only their shrinking. However, particle shrinking by surface erosion may suffice to explain the time-delayed generation and degradation of the 3–25  $\mu$ m size bin. Total numbers were higher with fluorescence

microscopy (Figure 1d) than with  $\mu$ -Raman microscopy (Figure 1b) because of the improved resolution and segmentation of particles within hetero- or homoagglomerates. These complementary techniques confirmed that fragments of all detectable sizes were further degraded and that there was no accumulation of detectable particles. We attribute the effective degradation of small fragments to the rate of enzymatic degradation scaling with the larger specific surface area of smaller fragments, as predicted for enzymatic surface erosion,<sup>33</sup> and confirmed experimentally.<sup>34</sup> Because of the scaling, there should be a certain size and time for which the outflow rate from this size (by erosion) exceeds the inflow rate of this size (by fragmentation of larger sizes), and the resulting size distribution should decrease toward smaller sizes; a peak should emerge. In our case, this peak was observed, specifically in the fraction of 25–75  $\mu$ m. The accumulation of nanoplastic fragments (below 1  $\mu$ m) would not be consistent with this model of the combined action of fragmentation and erosion, but nanoplastic by other mechanisms cannot be excluded by the present experimental data with a 3  $\mu$ m detection limit.

Enzymatic cleavage induces polymer chain scission, which should be observable in the molar mass distribution.<sup>33</sup> That parameter became measurable here selectively for the particles. We found that the polymer that constitutes the fragments resembled the original molar mass distribution (Figure 2a), even at 10 weeks, when 50% of the original polymeric carbon was converted into CO<sub>2</sub>. In contrast, Soxhlet extraction of compost, comprising the particles and polymer present in other forms (e.g., dissolved, adsorbed, bioassimilated), showed a gradually decreasing and polydisperse molar mass (Figure 2c). We thus identified depolymerization as driving force for shortened and more hydrophilic polymer chains to detach from particles because entanglement and van der Waals forces are reduced. Detached chains can be bioassimilated<sup>33</sup> and transformed into biomass<sup>35</sup> and CO<sub>2</sub>. We also identified the contribution of the different polymers of the compound by using GPC with refractive index (RI) and ultraviolet (UV) detection. The comparison between the molar mass of all polymers (GPC-RI, Figure 2c) and the molar mass of aromatic-aliphatic polyester (GPC-UV, Figure 2d) highlights the faster hydrolysis of PLA. This is in very good accord with the composition of the remaining fragments, shifting gradually from the original ecovio compound toward fragments with lower PLA content (Figure 2b). This shift was attributed to the rapid temperature-induced hydrolysis of PLA under the industrial composting conditions of 58 °C. It is worth noting that the shift of composition is not a “transformation”, because at the same time the particle count of all polyester fragments (Figure 1c) reduced to blank level. Fluorescence microscopy, which is not dependent on fitting to spectral libraries, provides additional evidence against the hypothesized generation of persistent microplastic because the count of all polymer fragments reduced to blank level (Figure 1d).

## ■ ENVIRONMENTAL IMPLICATIONS

Using the example of a specific, environmentally relevant plastic in industrial composting, the hypothesis of persistent microplastic generated via biodegradation was refuted.<sup>6–13</sup> No accumulation of particulate fragments of any detectable size was observed. The 25–75  $\mu$ m size range was the most pronounced peak of interim fragmentation. By metrics conversion of our limit of detection, it is estimated that less than 10<sup>–10</sup> of the mass of polymer was in 3–25  $\mu$ m fragments

at 90% CO<sub>2</sub>. Erosion seems to be dominant for such small particles.<sup>34</sup> The present case confirmed the expectation which Degli-Innocenti et al. had inferred from disintegration and mineralization rates, that compostable plastic should have a low microplastic emission potential.<sup>36</sup> In direct comparison we confirmed the high microplastic emission potential of LDPE.<sup>36</sup> Clearly the concept of microplastic emission potential or other fate models<sup>11,37,38</sup> must be refined with time-dependent particle sizes in both count and mass metrics. The analyses of a total of 200,000 particles identified a systematic and gradual shift of the polymer inside fragments to lower percentage of PLA, but neither  $\mu$ -Raman nor fluorescence microscopy found persistent fragments. Field tests which observed no fragments of compostable plastics in the output from aerobic composting plants<sup>39</sup> are consistent with our investigation of fragmentation kinetics. LDPE fragments persisted by our methods (Figure S6), and again field tests confirmed that assessment.<sup>9,40</sup> Fragments from incomplete degradation generated due to inappropriate processing, especially too short aerobic residence time in anaerobic/aerobic processes,<sup>41</sup> may enter agricultural fields. For the present case in that scenario, continued biodegradation in soil is expected due to the measured identity of partially degraded fragments (Figure 2a,b).<sup>11,42</sup> One can envision a follow-up investigation of particulate and nonparticulate polymer fractions by NMR, potentially supported by methods detecting isotopically labeled monomers.<sup>35,42</sup> Furthermore, fragmentation kinetics must be investigated in relation to copolymer composition, composting conditions, plastic shape, and up to entire bags and cups. Specifically, it has to be verified if the correlation of fragmentation kinetics with CO<sub>2</sub> evolution (Figure 1) also holds for 25  $\mu$ m thin films (in bags) or coatings (on paper cups). Scaling the results obtained here with 10-fold thicker granules by surface area,<sup>34</sup> the compost residence time required for the fragment numbers to return to blank level would scale 10-fold from 26 to 2.6 weeks for bags and paper cups, but this remains to be tested.

## ASSOCIATED CONTENT

### Supporting Information

The Supporting Information is available free of charge at <https://pubs.acs.org/doi/10.1021/acs.estlett.3c00394>.

Details on methods, CO<sub>2</sub> evolution of replicates, extraction protocol, blank control, stability controls, labeling control, identity and size of all plastics found, and LDPE control ([PDF](#))

## AUTHOR INFORMATION

### Corresponding Author

Wendel Wohlleben – BASF SE, 67056 Ludwigshafen, Germany; [orcid.org/0000-0003-2094-3260](https://orcid.org/0000-0003-2094-3260); Phone: +496216095339; Email: [wendel.wohlleben@bASF.com](mailto:wendel.wohlleben@bASF.com)

### Authors

Markus Rückel – BASF SE, 67056 Ludwigshafen, Germany  
Lars Meyer – BASF SE, 67056 Ludwigshafen, Germany  
Patrizia Pföhl – BASF SE, 67056 Ludwigshafen, Germany;  
Centre for Microbiology and Environmental Systems Science,  
University of Vienna, 1090 Vienna, Austria; Doctoral School  
in Microbiology and Environmental Science, University of

Vienna, 1030 Vienna, Austria; [orcid.org/0000-0002-1580-8833](https://orcid.org/0000-0002-1580-8833)

Glaucio Battagliarin – BASF SE, 67056 Ludwigshafen, Germany

Thorsten Hüffer – Centre for Microbiology and Environmental Systems Science, University of Vienna, 1090 Vienna, Austria; [orcid.org/0000-0002-5639-8789](https://orcid.org/0000-0002-5639-8789)

Michael Zumstein – Centre for Microbiology and Environmental Systems Science, University of Vienna, 1090 Vienna, Austria; [orcid.org/0000-0002-1099-5174](https://orcid.org/0000-0002-1099-5174)

Thilo Hofmann – Centre for Microbiology and Environmental Systems Science, University of Vienna, 1090 Vienna, Austria; [orcid.org/0000-0001-8929-6933](https://orcid.org/0000-0001-8929-6933)

Complete contact information is available at:  
<https://pubs.acs.org/10.1021/acs.estlett.3c00394>

## Author Contributions

The manuscript was written through contributions of all authors. All authors have given approval to the final version of the manuscript.

## Funding

P.P. was partially funded by BMBF (German Federal Ministry of Education and Research) within the InnoMat.Life project (funding no: 03XP0216X). M.Z., T.Hü., and T.Ho. were funded by the University of Vienna.

## Notes

The authors declare the following competing financial interest(s): W.W., M.R., L.M., G.B., and P.P. are employees of BASF, a company producing both conventional and biodegradable plastics, including the ecovio material.

## ACKNOWLEDGMENTS

We are grateful to Daniel Bahl, Florian Hornberger, Christoph Link, Christian Roth, and Marion Wagner for excellent lab work. We acknowledge guidance from Afsaneh Nabifar, the conception of the seminal experiments by Sarah Jessl (present address: TU Munich) and Eynat Biedermann, the synthesis contribution by Timo Witt (compounding with Lumogen Yellow), and the analytical contributions of Bastian Staal and Andrea Detels (GPC analysis). The Soxhlet protocol was optimized during the internship of Flora Wille (ETH).

## REFERENCES

- (1) European Environmental Agency (EEA). Report-No 04/2020; Bio-waste in Europe — turning challenges into opportunities (ISSN 1977-8449). 2020.
- (2) von Vacano, B.; Mangold, H.; Vandermeulen, G. W.; Battagliarin, G.; Hofmann, M.; Bean, J.; Künkel, A. Sustainable Design of Structural and Functional Polymers for a Circular Economy. *Angew. Chem.* **2022**, No. e202210823.
- (3) European Commission Directorate General for Environment; Hilton, M.; Geest Jakobsen, L.; Hann, S.; Favoino, E.; Molteno, S.; Scholes, R. *Relevance of biodegradable and compostable consumer plastic products and packaging in a circular economy*; Publications Office, 2020. DOI: [10.2779/497376](https://doi.org/10.2779/497376).
- (4) Eunomia. *Relevance of Conventional and Biodegradable Plastics in Agriculture. Final report to the European Commission DG Environment*; Contract No ENV.B1/FRA/2018/0002 Lot 1; 2021. <https://environment.ec.europa.eu/system/files/2021-09/Agricultural%20Plastics%20Final%20Report.pdf>.
- (5) Rieger, B.; Künkel, A.; Coates, G. W.; Reichardt, R.; Dinjus, E.; Zevaco, T. A. *Synthetic biodegradable polymers*; Springer Science & Business Media, 2012. ISBN 3642271545.

- (6) Liao, J.; Chen, Q. Biodegradable plastics in the air and soil environment: Low degradation rate and high microplastics formation. *Journal of Hazardous Materials* **2021**, *418*, No. 126329.
- (7) Qin, M.; Chen, C.; Song, B.; Shen, M.; Cao, W.; Yang, H.; Zeng, G.; Gong, J. A review of biodegradable plastics to biodegradable microplastics: Another ecological threat to soil environments? *Journal of Cleaner Production* **2021**, *312*, No. 127816.
- (8) Rillig, M. C.; Lehmann, A. Microplastic in terrestrial ecosystems. *Science* **2020**, *368* (6498), 1430.
- (9) Weithmann, N.; Möller, J. N.; Löder, M. G.; Piehl, S.; Laforsch, C.; Freitag, R. Organic fertilizer as a vehicle for the entry of microplastic into the environment. *Science advances* **2018**, *4* (4), No. eaap8060.
- (10) MacLeod, M.; Arp, H. P. H.; Tekman, M. B.; Jahnke, A. The global threat from plastic pollution. *Science* **2021**, *373* (6550), 61–65.
- (11) Rutgers, M.; Faber, M.; Waaijers-van der Loop, S. L.; Quik, J. T. K. Microplastics in soil systems, from source to path to protection goals: State of knowledge on microplastics in soil. *RIVM Report* **2022**, DOI: 10.21945/RIVM-2021-0224.
- (12) Chen, Y.; Leng, Y.; Liu, X.; Wang, J. Microplastic pollution in vegetable farmlands of suburb Wuhan, central China. *Environ. Pollut.* **2020**, *257*, No. 113449.
- (13) Zhang, G. S.; Liu, Y. F. The Distribution of Microplastics in Soil Aggregate Fractions in Southwestern China. *STOTEN* **2018**, *642*, 12–20.
- (14) Wei, X.-F.; Capezza, A. J.; Cui, Y.; Li, L.; Hakonen, A.; Liu, B.; Hedenqvist, M. S. Millions of microplastics released from a biodegradable polymer during biodegradation/enzymatic hydrolysis. *Water Res.* **2022**, *211*, No. 118068.
- (15) Weinstein, J. E.; Dekle, J. L.; Leads, R. R.; Hunter, R. A. Degradation of bio-based and biodegradable plastics in a salt marsh habitat: Another potential source of microplastics in coastal waters. *Mar. Pollut. Bull.* **2020**, *160*, No. 111518.
- (16) Sintim, H. Y.; Bary, A. I.; Hayes, D. G.; English, M. E.; Schaeffer, S. M.; Miles, C. A.; Zelenyuk, A.; Suski, K.; Flury, M. Release of micro- and nanoparticles from biodegradable plastic during in situ composting. *Science of The Total Environment* **2019**, *675*, 686–693.
- (17) Möller, J. N.; Löder, M. G.; Laforsch, C. Finding microplastics in soils: a review of analytical methods. *Environ. Sci. Technol.* **2020**, *54* (4), 2078–2090.
- (18) Pfohl, P.; Bahl, D.; Rückel, M.; Wagner, M.; Meyer, L.; Bolduan, P.; Battagliarin, G.; Hüffer, T.; Zumstein, M.; Hofmann, T.; et al. Effect of Polymer Properties on the Biodegradation of Polyurethane Microplastics. *Environ. Sci. Technol.* **2022**, *56*, 16873–16884.
- (19) Pfohl, P.; Roth, C.; Meyer, L.; Heinemeyer, U.; Gruendling, T.; Lang, C.; Nestle, N.; Hofmann, T.; Wohlleben, W.; Jessl, S. Microplastic extraction protocols can impact the polymer structure. *Microplastics and Nanoplastics* **2021**, *1* (1), 8.
- (20) Petrone, P.; Vismara, D. Separate collection of residential food waste in the city of Milan. *Müll und Abfall* **2014**, *5*, 253.
- (21) Arbeck, N.; Lehmann, J.; Sporrer, N.; Peintner, U. Abschlussbericht zum Modellprojekt, Praxistest Bio-Beutel – Kreislaufwirtschaft mit kompostierbaren Obst- und Gemüsebeuteln (Final report on the model project, practical test organic bags - circular economy with compostable fruit and vegetable bags), can be found under [https://www.carmen-ev.de/wp-content/uploads/2022/02/Abschlussbericht\\_Praxistest-Bio-Beutel.pdf](https://www.carmen-ev.de/wp-content/uploads/2022/02/Abschlussbericht_Praxistest-Bio-Beutel.pdf). Witzenhausen-Institut für Abfall, Umwelt und Energie GmbH 2022.
- (22) Kanthak, M.; Söling, F. Analysis of the use of compostable ecovio® organic waste bags. *Müll und Abfall* **2012**, *8*, 402–404.
- (23) Künkel, A.; Becker, J.; Börger, L.; Hamprecht, J.; Koltzenburg, S.; Loos, R.; Schick, M. B.; Schlegel, K.; Sinkel, C.; Skupin, G.; et al. Polymers, Biodegradable. *Ullman's Encyclopedia of Industrial Chemistry*; Wiley, 2016; 1, pp 1–29. DOI: 10.1002/14356007.n21\_n01.pub2.
- (24) Ruggero, F.; Gori, R.; Lubello, C. Methodologies for Microplastics Recovery and Identification in Heterogeneous Solid Matrices: A Review. *Journal of Polymers and the Environment* **2020**, *28* (3), 739–748.
- (25) ISO 14855: Determination of the ultimate aerobic biodegradability of plastic materials under controlled composting conditions — Method by analysis of evolved carbon dioxide; 2018.
- (26) Scopetani, C.; Chelazzi, D.; Mikola, J.; Leiniö, V.; Heikkinen, R.; Cincinelli, A.; Pellinen, J. Olive oil-based method for the extraction, quantification and identification of microplastics in soil and compost samples. *Science of The Total Environment* **2020**, *733*, No. 139338.
- (27) Möller, J. N.; Heisel, I.; Satzger, A.; Vizsolyi, E. C.; Oster, S. D. J.; Agarwal, S.; Laforsch, C.; Löder, M. G. J. Tackling the Challenge of Extracting Microplastics from Soils: A Protocol to Purify Soil Samples for Spectroscopic Analysis. *Environ. Toxicol. Chem.* **2022**, *41* (4), 844–857.
- (28) Tophinke, A. H.; Joshi, A.; Baier, U.; Hufenus, R.; Mitrano, D. M. Systematic development of extraction methods for quantitative microplastics analysis in soils using metal-doped plastics. *Environ. Pollut.* **2022**, *311*, No. 119933.
- (29) McDaniel, D. H. Acidity of Zinc Chloride Solutions. *Inorg. Chem.* **1979**, *18* (5), 1412.
- (30) Primpke, S.; Christiansen, S. H.; Cowger, W.; De Frond, H.; Deshpande, A.; Fischer, M.; Holland, E. B.; Meyns, M.; O'Donnell, B. A.; Ossmann, B. E.; et al. Critical Assessment of Analytical Methods for the Harmonized and Cost-Efficient Analysis of Microplastics. *Appl. Spectrosc.* **2020**, *74* (9), 1012–1047.
- (31) Prata, J. C.; da Costa, J. P.; Fernandes, A. J. S.; da Costa, F. M.; Duarte, A. C.; Rocha-Santos, T. Selection of microplastics by Nile Red staining increases environmental sample throughput by micro-Raman spectroscopy. *Science of The Total Environment* **2021**, *783*, 146979.
- (32) Accinelli, C.; Abbas, H. K.; Bruno, V.; Nissen, L.; Vicari, A.; Bellaloui, N.; Little, N. S.; Thomas Shier, W. Persistence in soil of microplastic films from ultra-thin compostable plastic bags and implications on soil Aspergillus flavus population. *Waste Management* **2020**, *113*, 312–318.
- (33) Haider, T. P.; Völker, C.; Kramm, J.; Landfester, K.; Wurm, F. R. Plastics of the Future? The Impact of Biodegradable Polymers on the Environment and on Society. *Angew. Chem., Int. Ed.* **2019**, *58* (1), 50–62.
- (34) Chinaglia, S.; Tosin, M.; Degli-Innocenti, F. Biodegradation rate of biodegradable plastics at molecular level. *Polym. Degrad. Stab.* **2018**, *147*, 237–244.
- (35) Zumstein, M. T.; Schintlmeister, A.; Nelson, T. F.; Baumgartner, R.; Woebken, D.; Wagner, M.; Kohler, H.-P. E.; McNeill, K.; Sander, M. Biodegradation of synthetic polymers in soils: Tracking carbon into CO<sub>2</sub> and microbial biomass. *Science Advances* **2018**, *4* (7), eaas9024.
- (36) Degli-Innocenti, F.; Barbale, M.; Chinaglia, S.; Esposito, E.; Pecchiari, M.; Razza, F.; Tosin, M. Analysis of the microplastic emission potential of a starch-based biodegradable plastic material. *Polym. Degrad. Stab.* **2022**, *199*, No. 109934.
- (37) Domercq, P.; Praetorius, A.; MacLeod, M. The Full Multi: An open-source framework for modelling the transport and fate of nano- and microplastics in aquatic systems. *Environmental Modelling & Software* **2022**, *148*, No. 105291.
- (38) Hüffer, T.; Praetorius, A.; Wagner, S.; Von Der Kammer, F.; Hofmann, T. Microplastic exposure assessment in aquatic environments: learning from similarities and differences to engineered nanoparticles. *Environ. Sci. Technol.* **2017**, *51* (5), 2499–2507.
- (39) Steiner, T.; Möller, J. N.; Löder, M. G.; Hilbrig, F.; Laforsch, C.; Freitag, R. Microplastic Contamination of Composts and Liquid Fertilizers from Municipal Biowaste Treatment Plants: Effects of the Operating Conditions. *Waste and Biomass Valorization* **2022**, *14*, 873–887.
- (40) Gui, J.; Sun, Y.; Wang, J.; Chen, X.; Zhang, S.; Wu, D. Microplastics in composting of rural domestic waste: Abundance, characteristics, and release from the surface of macroplastics. *Environ. Pollut.* **2021**, *274*, No. 116553.

(41) Steiner, T.; Zhang, Y.; Möller, J. N.; Agarwal, S.; Löder, M. G.; Greiner, A.; Laforsch, C.; Freitag, R. Municipal biowaste treatment plants contribute to the contamination of the environment with residues of biodegradable plastics with putative higher persistence potential. *Sci. Rep.* **2022**, *12* (1), 9021.

(42) Nelson, T. F.; Baumgartner, R.; Jaggi, M.; Bernasconi, S. M.; Battagliarin, G.; Sinkel, C.; Kunkel, A.; Kohler, H.-P. E.; McNeill, K.; Sander, M. Biodegradation of poly(butylene succinate) in soil laboratory incubations assessed by stable carbon isotope labelling. *Nat. Commun.* **2022**, *13* (1), 5691.

## □ Recommended by ACS

### Direct Measurement of Microplastics by Carbon Detection via Single Particle ICP-TOFMS in Complex Aqueous Suspensions

Lyndsey Hendriks and Denise M. Mitrano

APRIL 27, 2023

ENVIRONMENTAL SCIENCE & TECHNOLOGY

READ ▶

### Improved Reliability of Raman Spectroscopic Imaging of Low-Micrometer Microplastic Mixtures in Lake Water by Fractionated Membrane Filtration

Ziyan Wu, Haoran Wei, et al.

JUNE 12, 2023

ACS ES&T WATER

READ ▶

### A Novel Strategy to Directly Quantify Polyethylene Microplastics in PM<sub>2.5</sub> Based on Pyrolysis-Gas Chromatography-Tandem Mass Spectrometry

Peiru Luo, Zongwei Cai, et al.

FEBRUARY 09, 2023

ANALYTICAL CHEMISTRY

READ ▶

### Machine Learning Prediction of Adsorption Behavior of Xenobiotics on Microplastics under Different Environmental Conditions

Michael Taylor Bryant and Xingmao Ma

JUNE 26, 2023

ACS ES&T WATER

READ ▶

[Get More Suggestions >](#)